Lawrence Berkeley National Laboratory

Title
Magnetic Field Correction Methods for Hybrid Permanent Magnet and Superconducting Undulators

Permalink
https://escholarship.org/uc/item/7tr3p333

Journal
Synchrotron Radiation News, 31(3)

ISSN
0894-0886

Authors
Arbelaez, D
Leitner, M
Marks, S
et al.

Publication Date
2018-05-04

DOI
10.1080/08940886.2018.1460168

Peer reviewed

Magnetic Field Correction Methods for Hybrid Permanent Magnet and Superconducting Undulators

D. Arbelaez, M. Leitner, S. Marks, K. Mccombs, M. Morsch, H. Pan, S. O. Prestemon, T. Seyler & R. D. Schlueter

Published online: 24 May 2018.

Submit your article to this journal ↗

Article views: 79

View related articles ↗

View Crossmark data ↗

Magnetic Field Correction Methods for Hybrid Permanent Magnet and Superconducting Undulators

D. ARBELAEZ, M. LEITNER, S. MARKS, K. MCCOMBS, M. MORSCH, H. PAN, S. O. PRESTEMON, T. SEYLER, AND R. D. SCHLUETER
Lawrence Berkeley National Laboratory, Berkeley, California, USA

Introduction

This work describes tuning methods used at Lawrence Berkeley National Laboratory (LBNL) for hybrid permanent magnet and superconducting undulators (SCUs). The work on the hybrid permanent magnet undulators is intended for the LCLS-II project, where a large number of devices have to be built and tuned in an efficient manner [1]. Pole position adjustments have been successfully used for tuning of the European XFEL undulators [2–3]. The necessary features for these adjustments were built into the magnetic module design. For the LCSL-II project, a similar approach has been taken; however, more tuning methods have been considered in order to further reduce the gap dependence of errors in the undulators. The main focus of the work presented here is to analyze and design tuning methods that allow for effective error cancellation over a large gap range. The analysis tools that have been developed to rapidly determine the gap scaling of errors will be presented. The magnet module designs that incorporate these tuning methods will also be described.

For superconducting undulators, in order to reduce magnetic field errors, much of the focus is placed on accurate winding methodologies and machining processes (e.g., [4]). Nevertheless, for long devices, correction methods may still be necessary, depending on the allowed tolerances for the electron trajectories and phase errors. In a superconducting undulator, typical correction methods include a variety of on-board and decoupled end correctors, as shown in [4]. Here, a novel method is presented for trajectory correction and phase correction in the periodic section of the undulator. Different methods to correct local field errors have been previously proposed by several researchers; for example, the use of passive shim coils [5] and methods where the iron pole geometry is modified [6]. Active methods have also been proposed that combine trim coils [7] and active switching networks [8] in order to perform in-situ corrections of errors at specific locations in a device. This concept was first pursued using the high-temperature superconductor YBCO [9]. The use of YBCO has the advantage that the superconductor is available in the form of a thin tape readily available from commercial sources. In this work, a method is presented where YBCO tapes are patterned into single-turn coils that can be actively switched using heaters. This allows for in-situ correction of errors at desired locations along the length of the undulator. The feasibility of this method has been demonstrated during the test of a Nb_3Sn undulator that was built at LBNL and tested at Argonne National Lab (ANL) as part of a collaboration between the Stanford Linear Accelerator (SLAC), ANL, and LBNL [10].

In the following text, the methods used for analyzing errors and tuning methods for hybrid undulators will be described. The design of the magnetic modules for the LCLS-II project, which incorporate various tuning methods, will be presented. This will be followed by a description of the superconducting undulator tuning scheme. The fabrication methods and test results for the SCU tuning scheme will also be presented.

Analysis of hybrid magnets

An analysis tool for determining the gap-dependent response of various undulator errors and tuning methods has been developed. The analysis approach used here follows the theory developed by Halbach for the analysis of insertion devices [11]. This analysis approach does not account for finite permeability and saturation effects; however, it allows for fast analysis of many different types of errors and tuning methods. This leads to a useful tool for understanding the gap dependence of different types of errors and aids in the design of tuning methods. An important advantage of this method is that it allows for direct solution of perturbation problems without subtracting two slightly perturbed solutions, which requires substantially finer meshes.

An overview of the analysis of hybrid magnets composed of permanent magnet (PM) material and infinite permeability field-shaping surfaces is first presented. For a more detailed review of this approach, the reader is referred to the work by Schlueter [12]. In this model, the PM material is equivalently replaced by charge sheets located at appropriate surfaces on the PM block. This is an exact model for uniformly magnetized PM blocks with relative permeability, μ = 1. Figure 1 shows a schematic of the approach followed in the modeling of hybrid magnets. On the left, the hybrid magnet model is shown, which is represented by two iso-scalar potential surfaces with a nearby charge, Q. Here, surface 2 is a reference surface where the scalar potential is chosen to be V = 0 without loss of generality. A solution to this problem, which satisfies Maxwell's equations in space and has zero net flux entering surface 1, is desired. The solution to this problem can be decomposed into direct and indirect fields. The direct fields are defined as those that emanate from the charge Q and are deposited onto surfaces 1 and 2 when both surfaces are on zero scalar potential. Indirect fields are generated by the difference in scalar potential between surfaces 1 and 2 with the charge Q no longer present.
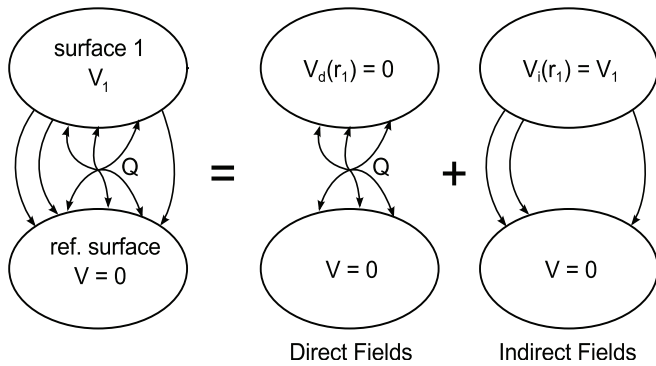
Figure 1: Hybrid magnet analysis with decomposition of fields into direct and indirect contributions. The direct fields are defined as those that emanate from the charge Q (from PM material) and are deposited onto zero scalar potential surfaces. Indirect fields are generated by the difference in scalar potential between surfaces 1 and 2 with no charge present.

Using the decomposition of direct and indirect fields, a solution to the hybrid magnet model can be obtained by requiring that there is zero net flux into surface 1. This can be described by $CV_1 + \Phi_d = 0$, where C is the capacitance between the two surfaces, Φ_d is the direct flux into the pole due to the permanent magnet, and V_1 is the equilibrium surface potential. The term CV_1 represents the indirect flux into surface 1 (see Figure 1 (right)), where the capacitance, C, is a proportionality constant that depends only on the geometry of the problem. The capacitance is calculated by putting surface 1 on an arbitrary potential, V_0 (with the reference surface on zero potential and zero charges), and calculating the flux into surface 1 ($C = flux/V_0$). The direct flux, Φ_d, is determined by solving for the flux through surface 1 with the charges present and both surfaces on zero scalar potential. This can be generalized to multiple surfaces, where the equation $[C]\{V\} + \{\Phi_d\} = 0$ defines the flux balance. In this case, [C] is an N by N matrix (for N poles) and $\{V\}$ and $\{\Phi_d\}$ are vectors with N components. This analysis method will be used in the following sections for the analysis of hybrid undulators.

Hybrid undulator error and tuning analysis

The hybrid magnet theory described earlier is used to perform various analyses for the LCLS-II hybrid undulators. A dedicated Boundary Element Method (BEM) code has been developed using Fortran to calculate the capacitance matrix and the direct flux into the poles of the hybrid undulator. Using the BEM calculation, the capacitance matrix for the hybrid undulator is determined by setting one pole on non-zero scalar potential, V_0 (with all others on zero), and evaluating the normalized flux through all of the poles. This gives one column of the capacitance matrix. The process is repeated for all of the poles in order to fill the entire matrix. The direct field can be calculated by including the PM surfaces with their specified charge densities, with all poles on zero scalar potential. Figure 2 shows a visualization of this type of calculation. The flux into the poles is calculated for given charge sheets that represent two cylindrical permanent magnets.

The method for determining the magnetic field perturbations from various possible fabrication errors, as well as the signatures that can be generated by the proposed tuning methods, are now analyzed. For a more detailed description of the analysis method, the reader is referred to [13]. For this analysis, two types of perturbations are considered: (1) PM direct flux contributions; and (2) geometric contributions. Including these perturbations, the flux balance equation can be written as:

$$([C] + [\delta C])(\{V\} + \{\delta V\}) + (\{\Phi_d\} + \{\delta \Phi_d\}) = 0,$$

where $\{\delta \Phi_d\}$ is the direct flux perturbation and $[\delta C]$ is the variation in capacitance due to geometric perturbations. Using the nominal flux balance, $[C]\{V\} + \{\Phi_d\} = 0$, and neglecting the higher-order term, the perturbation flux balance can be written as:

$$[C]\{\delta V\} = -[\delta C]\{V\} - \{\delta \Phi_d\},$$

where $\{\delta \Phi_d\}$ and $[\delta C]\{V\}$ are pole flux perturbations, and $\{\delta V\}$ is the pole potential variation that is necessary in order to maintain the direct
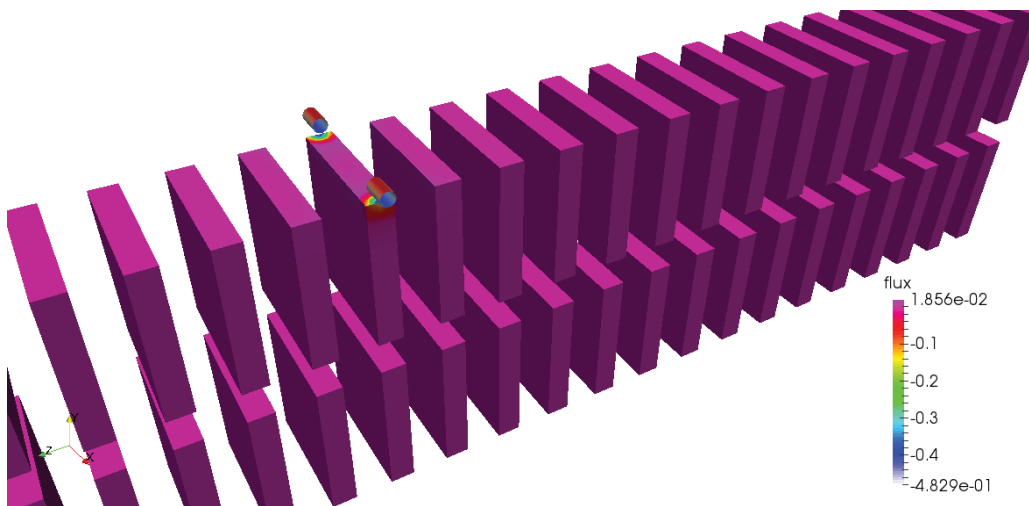

Figure 2: This graphic shows an example of a boundary element solution for the analysis of hybrid undulators. The open-source program ParaView is used for the visualization of the potentials and flux, as shown in this figure.
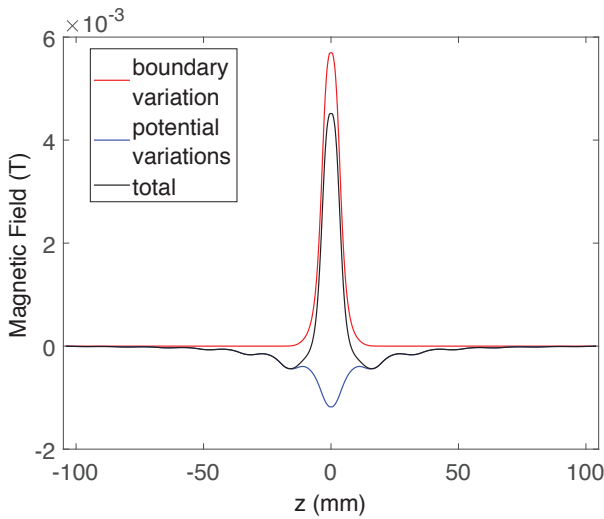
Figure 3: This plot shows the magnetic field signature from a vertical pole position error/tuning method (position perturbation = 25 μm). The red line represents the contribution from the boundary variation, while the blue line represents the contribution from the potential variations ({δV}).

and indirect flux balance. $\{\delta\Phi_d\}$ is given by the direct flux into the poles from the excess charges. $[\delta C]\{V\}$ is determined by setting the potential of the perturbed pole surface to $\partial V/_{\partial x}\delta x$ (while all other surfaces are set to $V = 0$), where V is the potential solution when all poles are on their nominal potential (i.e., $\{V\} = \{-V0, V0, V0, -V0, -V0, \ldots\}$ using the numbering convention from Figure 3, and δxis the magnitude of the geometric perturbation. The total error on the undulator axis is then given by the sum of the flux perturbation contributions, $\{\delta\Phi_d\}$ or $[\delta C]\{V\}$, and the variation in the potential of the poles $\{\delta V\}$. Figure 3 shows an example for the calculated magnetic field from a vertical pole position error/tuning method. In the figure, the red line represents the contribution from the boundary variation, while the blue line represents the contribution from the potential variations ($\{\delta V\}$). Note that, for this case, the potential perturbations, $\{\delta V\} = -[C]^{-1}([\delta C]\{V\})$, arise only from the flux perturbation $[\delta C]\{V\}$, since there is no excess direct PM flux. The red line in Figure 3 is the on-axis field when the perturbed surface is set to the potential $\partial V/_{\partial x}\delta x$, while $[\delta C]\{V\}$ is the flux through the poles when this boundary condition is applied. The perturbation analysis has been performed on a number of errors and/or tuning methods, including the following: vertical pole position (error/tuning), axial pole position (error), pole thickness (error), pole height (error), pole width (error), PM block strength (error), PM block angle (error), PM rotors and slugs (tuning), and pole cant (error/tuning).

Magnet module design for LCLS-II

The LCLS-II magnet modules incorporate different tuning features in order to obtain better correction of errors over the entire gap range. Figure 4 shows the magnet module designs for the soft X-ray (SXR) beamline in the top picture and for the hard X-ray (HXR) beamline in the bottom picture. The SXR and HXR designs both include pole posi-

tion adjustments and slots for permanent magnet materials. The SXR design uses a flexure for the pole adjustment, while the HXR design uses set screws to position the poles, which is a lower-cost approach. For the SXR module, permanent magnet rotors are used to modify the potential of the nearby pole. Magnet slugs are also used in this design, as well as in the HXR modules. Figure 5 shows the magnetic first integral as a function of gap for pole and rotor adjustments for the SXR undulator. The solid lines show the measured field integral for rotor and pole adjustments, while the dashed lines show the calculated field integral using the model presented earlier. The modeling results accurately predict the difference in gap dependence between the pole and rotor adjustments. However, saturation effects start to dominate at small gaps, which give a deviation from the ideal modeling results. The main advantage of the modeling approach presented here is that the gap scaling for many tuning and error signatures can be obtained in a computationally inexpensive manner. Deviations from ideal behavior must then be measured for application to tuning algorithms.
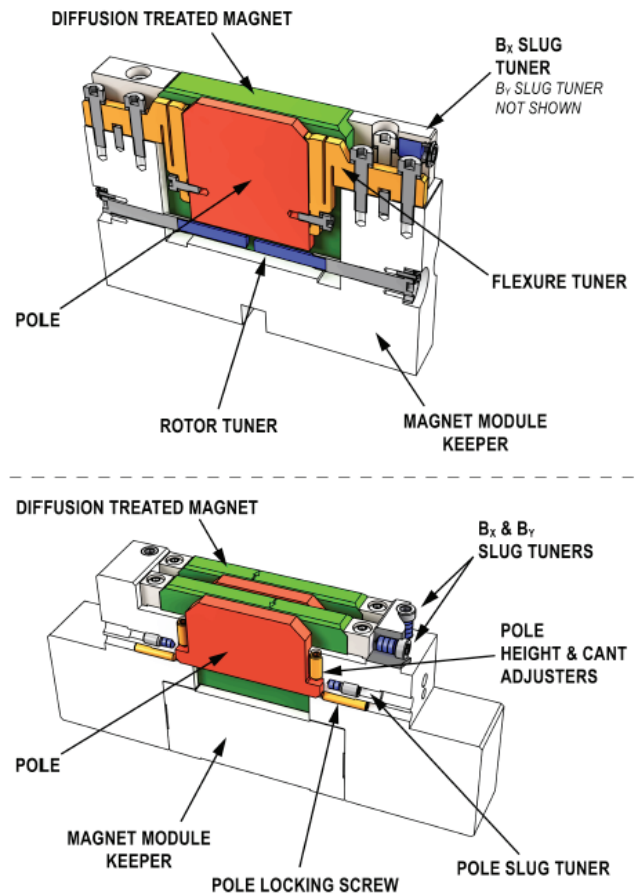

Figure 4: The LCLS-II magnet modules incorporate different tuning features in order to obtain better correction of errors over the entire gap range. The SXR (top) and HXR (bottom) designs both include pole position adjustments and slots for permanent magnet materials.
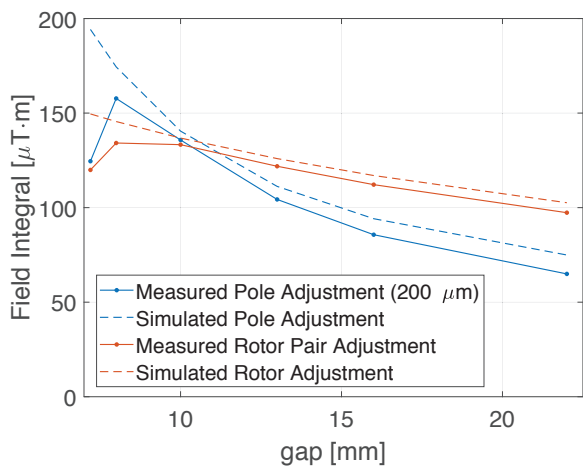
Figure 5: The tuning signatures for the SXR undulator have been calculated and measured experimentally. The plot above shows the gap dependence for vertical field adjustments that are achieved by adjusting the vertical pole position or by inserting permanent magnet rotors into the module.

Superconducting undulator field correction system

The correction of local field errors in superconducting undulators is complicated by the lack of easy access to these devices, since they must operate in a cryostat. The tuning scheme presented here uses single-turn coils and superconducting switches in order to correct the magnetic field at specific locations along the periodic section of the device. All of the single-turn coils are wired in series such that, when activated, the current through all coils is the same. The coils can be activated by using heater switches that divert the current from a bypass path to the individual single-turn coils. Therefore, the correction is performed with a single variable current source and variable on/off single-turn coils which can be activated at the desired locations along the length of the device. This type of concept has the advantage that it can be used to
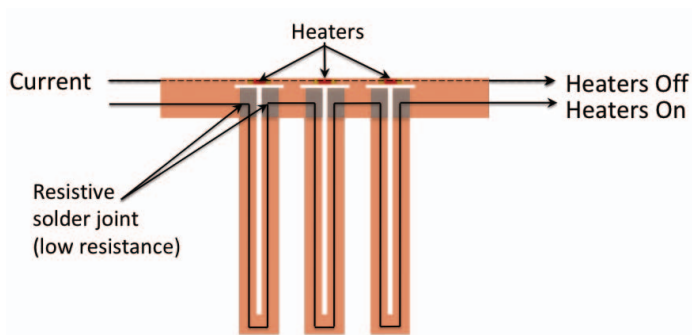

Figure 6: This diagram shows the switching concept for local field correction of superconducting undulators, using YBCO superconducting tapes, resistive joints, and switching heaters. When the heaters are off, the current bypasses the single-turn coils. When a heater is turned on, the majority of the current (>99%) now goes through the single-turn coil for undulator field correction.
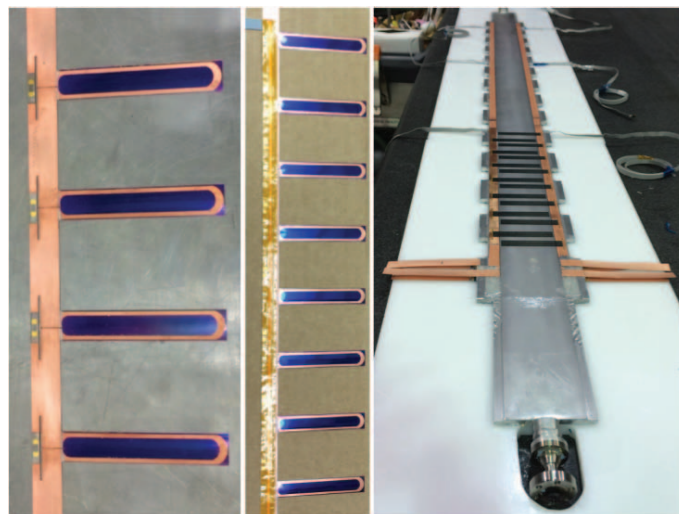

Figure 7: The YBCO corrector segments are fabricated using lithography and etching to generate the loops, soldering to adhere the heaters and create the low-resistance electrical connections, and laser cutting to separate the ends of the current loops. The segments are subsequently wired with flexible circuit boards (middle) and adhered to the surface of the vacuum chamber (right).

tune the undulator in-situ, while magnetic measurements are performed on the device.

The single-turn correction coils are placed on the each side of the vacuum chamber under the undulator poles. The coils are placed in a pattern that allows for positive and negative kick corrections, as well as positive and negative phase error corrections. A switching scheme that uses YBCO tapes with resistive joints and active heaters has been developed for the tuning of the undulator prototypes. Figure 6 shows a diagram of this concept, which includes the main tape, the soldered single-turn coil tapes (low resistance joints), and the switching heaters. As is shown in the figure, when the heaters are off, the current bypasses the single-turn coils, since the top path is superconducting. Once a heater is turned on, a majority of the current (>99%) now goes through the single-turn coil for undulator field correction. This is the case since the resistance of the top path in the normal state is much higher than the resistance of the joint between the two soldered tapes.

In order to incorporate the correction system for the undulator test, the YBCO correctors must be attached to the vacuum chamber. A vacuum bag process is used to adhere the tapes to the vacuum chamber in order to ensure an even surface with a thin glue line. The corrector system adds approximately 0.2 mm to each side of the vacuum chamber. Thin and flexible circuit boards were designed in order to carry the current for the heater activation. This helps minimize the space required for the correction system. The correctors are made in segments with eight correction loops, and solder joints are made between corrector segments. Figure 7 (left) shows the segments, which are fabricated using lithography and etching to generate the loops, soldering to adhere the heaters and create the low-resistance electrical connections, and

laser cutting to separate the ends of the current loops. The segments are subsequently wired with the flexible circuit boards (middle) and adhered to the surface of the vacuum chamber (right).

Superconducting undulator field correction test

A Nb_3Sn undulator was fabricated at LBNL and tested at ANL as part of the superconducting undulator collaboration with ANL and SLAC. The tuning system was part of the deliverable from LBNL, and its performance was evaluated during the Nb_3Sn undulator test. Figure 8 (top) shows the magnetic field generated due to the activation

of six correctors along the length of the device at 100 A. The shaded area represents the locations where correctors were available. Due to some fabrication issues and time constraints, the correctors were applied to the first and last third of the vacuum chamber, and they were only present on one side of the chamber. Therefore, the correctors were available over only two-thirds of the device at one-half of their nominal strength. The bottom graphic in Figure 8 shows the change in phase error obtained from the applied corrections. It can be seen that, even with the limited locations and strength, the rms phase error is reduced from 9.2° to 5.4°. This successful test demonstrates the ability to correct the magnetic field in a superconducting undulator with an active system.
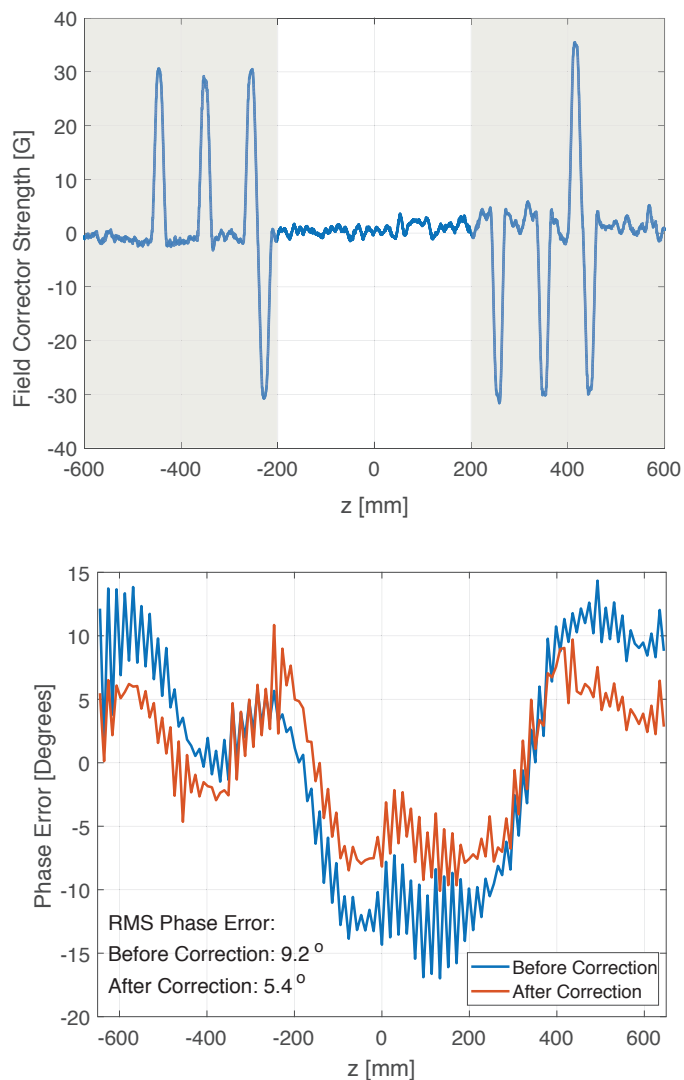
Conclusion

The analysis and design of efficient tuning methods are essential for FEL facilities where many undulators must be tuned in a large production. This has been an important focus for the LCLS-II project, which uses variable gap hybrid permanent magnet undulators. Efficient analysis tools have been developed in order to understand the effect of fabrication errors and the gap dependence of tuning methods for these undulators. This led to the design of magnet modules with features incorporated for efficient tuning of these undulators. For superconducting undulators, the lack of access makes tuning of these devices difficult. A tuning method using commercial YBCO tapes and activation heaters has been developed and demonstrated. This is the first demonstration of active correction of local errors on a full-length superconducting undulator.

Figure 8: The field correctors are activated at specific locations in order to reduce the phase errors in the Nb_3Sn undulator. The top graphic shows the change in magnetic field after activating the correctors. The shaded area represents the locations where correctors were available. The bottom graphic shows the change in phase error obtained from the applied corrections.

References

1. M. Leitner et al., *Proceedings of IPAC2017*, Copenhagen, Denmark (2017).
2. J. Pflueger et al., *Proceedings of FEL2013*, New York, NY (2013).
3. U. Englisch, Y. H. Li, and J. Pflueger, *Proceedings of FEL2012*, Nara, Japan (2012).
4. Y. Ivanyushenkov et al., *Physical Review Accelerators and Beams* **20**, 100701 (2017).
5. D. Wollmann et al., *Physical Review Accelerators and Beams* **12**(4), 040702-1–040702-6 (2009).
6. S. Chunjarean et al., *Superconductor Science and Technology* **24**(5), 055013-1–055013-7 (2011).
7. S. O. Prestemon et al., *IEEE Transactions of Applied Superconductivity* **15**(2), 1236–1239 (2003).
8. A. Madur et al., *Proceedings of AIP Conferences* **1234**, 552–555 (2010).
9. D. Arbelaez et al., *IEEE Transactions of Applied Superconductivity* **23**(3), 4100104 (2013).
10. P. Emma et al., *Proceedings of FEL2014*, Switzerland, THA03, 649–653 (2014).
11. K. Halbach, *Lawrence Berkeley National Laboratory Report*, LBL-034 (1989).
12. R. D. Schlueter, *Lawrence Berkeley National Laboratory Report,* LBL-36839 (1995).
13. D. Arbelaez et al., *Proceedings of FEL2011*, WEPA24 (2011).